Cloning, Expression, and Functional Analysis of Rat Liver Cytosolic Inorganic Pyrophosphatase Gene and Characterization of its Functional Promoter

HAREKRUSHNA PANDA, RAVI S. PANDEY, PRIYA R. DEBATA, AND PRAKASH C. SUPAKAR

Institute of Life Sciences, Bhubaneswar, India

Inorganic pyrophosphate (PPi) is formed in several metabolic processes and its hydrolysis by the ubiquitously expressed enzyme inorganic pyrophosphatase (iPPase) is essential for the reactions to proceed in the direction of biosynthesis. Recently, we have reported differential expression and activity of cytosolic iPPase in rat liver with aging. In this article we report the cloning of the coding region of rat liver cytosolic iPPase gene in a bacterial expression vector, its expression, purification, and functional analysis by in-gel enzyme assay. SDS-PAGE and Western blot analysis of this expressed protein revealed that its molecular weight (MW) is ~33 kDa, while in-gel assay showed that it is functionally active just as the liver cytosolic iPPase. We have determined the genomic organization of this gene by genome blast approach. We have also cloned and characterized its proximal ~1 kb functional promoter (−1009 to +82) by transient transfection and luciferase assay of different 5′-deleted iPPase promoter–luciferase constructs and also established its transcription start site by primer extension analysis, along with protein–DNA interaction studies for a few putative transcription factor binding sites.

Key words: Inorganic pyrophosphatase; Gene expression; In-gel assay; Transcription start site; Protein–DNA interaction

INTRODUCTION

The formation of large amounts of inorganic pyrophosphate (PPi) as a by-product of numerous synthetic reactions such as RNA, DNA, oligosaccharide biosynthesis, fatty acid, and amino acid activation in nearly all living tissues makes the molecule very interesting for its metabolic study. PPi regulates certain intracellular and extracellular functions, as a substrate, phosphate donor (17), and as a chelator of several divalent metal ions, thus regulating those enzymes that are activated or inhibited by such metal ions (9,29). Therefore, the maintenance of a steady-state level of PPi is essential for regulation of metabolic reactions.

Dysregulated cellular PPi production, degradation, and transport all have been associated with diseases (19) and PPi appears to directly mediate specific disease manifestations (26). The intramitochondrial volume and its adenine nucleotide content are regulated by inorganic pyrophosphate (4). The PPi-utilizing metabolic enzyme, phosphofructokinase (16), and other intracellular proteins like myosine magnesium ATPase and F1-ATPase (15) have been found to be sensitive to PPi dysregulation. Pyrophosphate also forms strong complexes with iron and enhances iron transfer between transferrin, ferritin, and tissues (6).

The rather large amount of PPi that is produced in the liver during synthesis of urea, RNA, DNA, protein, glycogen, and fatty acid activation has been assumed to be hydrolyzed by inorganic pyrophosphatase (7). Systematic fractionation of subcellular com-

ponents has revealed that 92% of total iPPase activity of rat liver is in the cytosol and about 4.5% is present in mitochondria. However, only negligible iPPase activity is found in the membrane fractions, isolated by sucrose gradient (21). These findings indicate that cytosol is the major and mitochondria the minor locus for intracellular iPPase activity. In the liver, cytosolic iPPase (EC 3.6.1.1) is the major player in PPi hydrolysis. Thus, the study of expression, activity, and transcriptional regulation of this enzyme in liver would be an important finding in understanding its physiological role in PPi metabolism.

While studying differential gene expression during aging using differential display PCR (DD-PCR), we found a cDNA band (~196 bp) whose expression level was higher in old animals (aged 24 months) than their adult counterparts (aged 4 months) and this differential expression was also confirmed by Northern blot analysis (18). Cloning, sequencing, and blast search analysis of this cDNA band revealed that it has significant sequence homology with rat prostate cytosolic inorganic pyrophosphatase mRNA (Gen Bank accession number BC099794) and predicted rat inorganic pyrophosphatase mRNA (GenBank accession number XM_215416.2). Comparative sequence analysis indicated that this predicted rat inorganic pyrophosphatase mRNA has a well-defined open reading frame (ORF) and showed 100% sequence identity with the rat prostate inorganic pyrophosphatase mRNA.

In order to validate DD-PCR finding we have cloned the coding region of rat liver cytosolic iPPase gene, based on the RT-PCR primers designed from predicted rat iPPase mRNA in a bacterial expression system to determine whether it codes for a viable protein and whether this expressed protein is functionally active. We have cloned the 870-bp coding region of rat liver cytosolic iPPase in bacterial expression vector pTrcHis TOPO TA and expressed the recombinant protein by IPTG induction. SDS-PAGE and Western blot analysis of this N-terminal His-tagged recombinant protein revealed that the apparent molecular weight of the expressed rat liver cytosolic iPPase protein is ~33 kDa. In-gel assay for this recombinant protein showed that it is functionally active just as the liver cytosolic iPPase. Further, for the first time we have cloned and characterized the proximal ~1 kb functional promoter (−1009 to +82) of this ubiquitously expressed enzyme, established its transcription start site, found out the putative transcription factor binding sites, and carried out protein–DNA interaction studies for a few putative transcription factor binding sites, which may help in understanding the molecular mechanism underlying the transcriptional regulation of this gene.

MATERIALS AND METHODS

Cloning, Expression, and Purification of Rat Liver Cytosolic iPPase and Determination of its Molecular Weight

In order to detremine the coding region of rat liver cytosolic iPPase gene, the following RT-PCR primers were designed from predicted iPPase mRNA sequence. Sense primer XIPF (5′-ATGAGCAGCTT CAGCAGC-3′) and antisense primer XIPR (5′-GGAATCGCATCAGTTTTTCTG-3′) were designed and used for RT-PCR to get the coding region of rat liver cytosolic inorganic pyrophosphatase gene, taking rat liver cDNA as template. PCR amplification was carried out for 35 cycles under the following standard conditions: denaturation (94°C for 40 s), annealing (60°C for 40 s), extension (68°C for 2 min), followed by a final extension (68°C for 8 min) using 1 unit of platinum *Taq* DNA polymerase (Invitrogen, USA). The RT-PCR gave a 879-bp product, which was sequenced and subsequently cloned into pTrcHis TOPO TA expression vector (Invitrogen) according to the manufacturer's instructions. The recombinant protein was expressed in *Escherichia coli* (TOP10 cells, Invitrogen) by IPTG induction and its size was checked by SDS-PAGE and Western blot analysis using anti-His-HRP-conjugated antibody (Invitrogen). The N-terminal 6× His-tagged recombinant protein was purified by affinity chromatography using Ni-NTA column (Invitrogen) under denaturing condition according to the manufacturer's instructions. The purified denatured recombinant protein was renatured (8) and was used for in-gel assay to study its enzyme activity.

In-Gel iPPase Assay

To determine enzyme activity of bacterially expressed rat liver cytosolic iPPase in comparison to rat liver cytosolic iPPase, whole cell lysates (WCL) were prepared from IPTG-induced bacteria cells harboring the iPPase expression vector and also from the rat liver tissue. In brief, samples were homogenized in ice-chilled iPPase buffer (50 mM Tris-Cl, 3 mM $MgCl_2$, 0.2 mM EGTA, pH 7.6), centrifuged at 2500 × *g* for 5 min at 4°C, and the supernatant was used for in-gel analysis after determination of its protein content by Bradford reagent (Sigma, USA). The WCL (bacterial and liver WCL) and the purified renatured expressed rat liver cytosolic iPPase were solubilized in 3× protein loading buffer (20% v/v glycerol, 190 mM Tris-Cl, pH 6.8, 0.025% bromophenol blue) and electrophoresed on an 8% nondenaturing polyacrylamide gel at 120 V for a period of 6 h. After electrophoresis, the gel was briefly rinsed with 10 gel

TABLE 1
OLIGONUCLEOTIDE DUPLEXES USED IN ELECTROPHORETIC MOBILITY SHIFT ASSAY (EMSA)

Position of Putative Transcription Factor Binding Site on iPPase Promoter	Sequence
iPPase Sp1 (−102 to −82)	5′-GAC<u>GGGGCGGGGC</u>AGGGTGCA-3′ 3′-CTGCCCCGCCCCGTCCCACGT-5′
iPPase Sp1 (−158 to −138)	5′-TGTACT<u>GGGGGCGGGGC</u>GTGA-3′ 3′-ACATGACCCCCGCCCCGCACT-5′
iPPase NF-κB (−736 to −717)	5′-CTCCT<u>GGGCCTTCCC</u>AGAGC-3′ 3′-GAGGACCCGGAAGGGTCTCG-5′

The core consensus transcription factor binding site on the sense strand is underlined.

volumes of distilled water, preincubated in the iPPase buffer for 15 min to equilibrate the gel, replaced by freshly prepared iPPase buffer containing 4 mM substrate (tetra sodium pyrophosphate), and again incubated for 30 min. All incubations were carried out at 37°C with continuous gentle agitation. The gel was briefly rinsed in distilled water and the released phosphate was precipitated using phosphate precipitation reagent (1% w/v ammonium molybdate, 1% w/v triethylamine, and 1M HNO_3) (23). The precipitated phosphate band in the gel was photographed as soon as it appeared. The specificity of iPPase activity in this assay was confirmed by reported iPPase inhibitors like $CaCl_2$ and NaF (data not shown).

Cloning of 1.009 kb Rat Cytosolic iPPase Promoter

Comparative sequence analysis revealed that the predicted rat inorganic pyrophosphatase mRNA has 100% sequence identity with the reported rat prostate cytosolic mRNA sequence. Therefore, a genome blast was performed using available rat prostate cytosolic mRNA sequence against the whole rat genome in order to find out the genomic organization of this gene. Based on the genome blast result, following primers were designed: sense primer CIPF (5′-TGAGACAGAGTCTCATGGAGTCC-3′) corresponding to the −1550 to −1527 region, and antisense primer CIPR (5′-GAGAGTCTGGAATGAATGGGTGAC-3′) corresponding to the +195 to +172 region of predicted
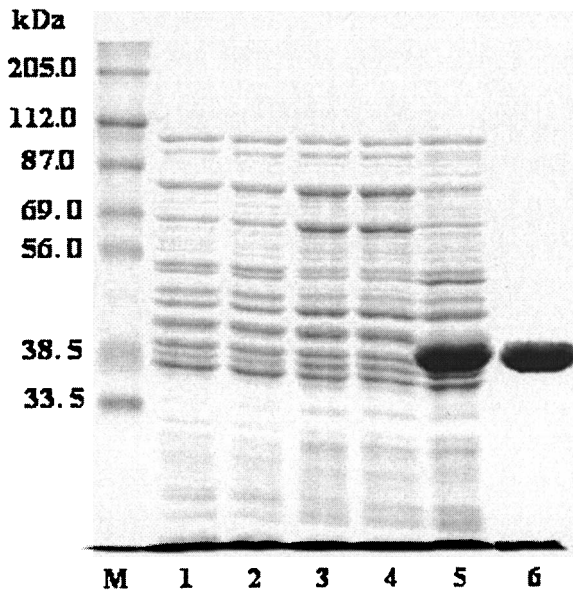

Figure 1. SDS-PAGE analysis of expressed His-tagged rat liver cytosolic inorganic pyrophosphatase. Lane M: molecular weight marker in kDa. Whole cell lysate of: lane 1, *E. coli* cells; lane 2, 15-h IPTG-induced *E. coli* cells transformed with self-ligated expression vector pTrcHis TOPO TA ; lane 3, 15-h IPTG-induced *E. coli* cells transformed with expression vector containing rat liver cytosolic iPPase coding region out-of-frame with the vector; lane 4, 0-h IPTG-induced *E. coli* cells transformed with expression vector containing rat liver cytosolic iPPase coding region in-frame with the vector; lane 5, 15-h IPTG-induced *E. coli* cells transformed with expression vector containing rat liver cytosolic iPPase coding region in-frame with the vector; lane 6, Ni-NTA purified recombinant rat liver cytosolic iPPase protein by denaturing method. In each lane 10 μg of protein was taken except for lane 6, where 5 μg purified recombinant protein was used.

Figure 2. Western blot analysis of expressed His-tagged rat liver cytosolic inorganic pyrophosphatase using anti-His-HRP-conjugated antibody. Whole cell lysate of: lane 1, *E. coli* cells; lane 2, 15-h IPTG-induced *E. coli* cells transformed with self-ligated expression vector pTrcHis TOPO TA ; lane 3, 15-h IPTG-induced *E. coli* cells transformed with expression vector containing rat liver cytosolic iPPase coding region out-of-frame with the vector; lane 4, 0-h IPTG-induced *E. coli* cells transformed with expression vector containing rat liver cytosolic iPPase coding region in-frame with the vector; lane 5, 15-h IPTG-induced *E. coli* cells transformed with expression vector containing rat liver cytosolic iPPase coding region in-frame with the vector; lane 6, Ni-NTA purified recombinant rat liver cytosolic iPPase protein by denaturing method. In each lane 10 μg of protein was taken except for lane 6, where 5 μg purified recombinant protein was used.
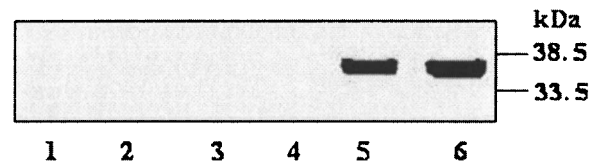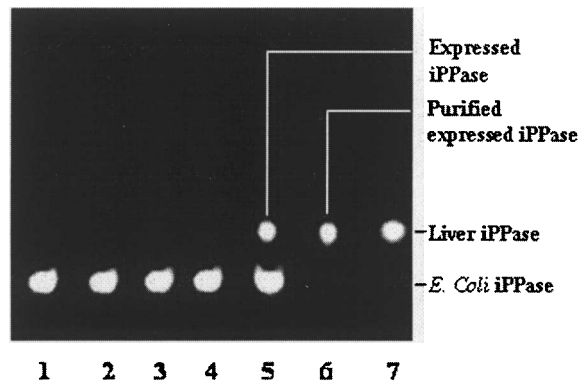
Figure 3. Study of functional activity of expressed rat liver cytosolic iPPase by in-gel assay. Whole cell lysate protein (12 μg) of: lane 1, *E. coli* cells; lane 2, 15-h IPTG-induced *E. coli* cells transformed with self-ligated expression vector pTrcHis TOPO TA; lane 3, 15-h IPTG-induced *E. coli* cells transformed with expression vector containing rat liver cytosolic iPPase coding region out-of-frame with the vector; lane 4, 0-h IPTG-induced *E. coli* cells transformed with expression vector containing rat liver cytosolic iPPase coding region in-frame with the vector; lane 5, 15-h IPTG-induced *E. coli* cells transformed with expression vector containing rat liver cytosolic iPPase coding region in-frame with the vector. Lane 6: 5 μg of Ni-NTA column purified renatured rat liver cytosolic iPPase. Lane 7: 40 μg of rat liver WCL. Lanes 1–4 show only endogenous iPPase activity of *E. coli*. Lane 5 shows activity of expressed rat liver iPPase as well as endogenous *E. coli* iPPase. Lane 6 shows activity of purified bacterially expressed rat liver iPPase. Lane 7 shows native rat liver iPPase.

iPPase gene. Using rat liver genomic DNA and the above-mentioned primers, a PCR product of ~1745 bp was obtained, which was taken as template for the second round of nested PCR using sense primer CIPF$_1$ (−1009 to −986; 5′-ATAGTCTCATACTG GAGCTCAGGC-3′) and antisense primer CIPR$_1$ (+82 to +62; 5′-GGTGTCCGAGATGTGCCTGTG-3′), giving a PCR product of 1091 bp. PCR amplification was carried out for 35 cycles using step cycle 94°C for 1 min, 63°C for 1 min, 68°C for 2 min followed by final extension at 68°C for 8 min, taking 1 unit of platinum *Taq* DNA polymerase. This PCR product was cloned into pGEM-T vector (Promega, USA), sequenced, and was used as template DNA for construction of iPPase reporter constructs.

Primer Extension Analysis

A 21-nucleotide-long primer IPER, with the sequence 5′-GGTGTCCGAGATGTGCCTGTG-3′, which is complementary to the +82 to +62 region of iPPase predicted exon-1, was used for primer extension analysis. Briefly, 200 fmol of 5′-end-labeled IPER primer was annealed with 50 μg of total RNA at 60°C for 1 h, cooled to room temperature, and reverse transcribed at 42°C for 1 h using primer extension system (Promega) according to the manufacturer's instruc-

tions. The same primer was used for the sequencing reactions of cloned iPPase promoter containing exon-1. Sequencing reactions and primer extension product were separated, side by side on a 7.5% polyacrylamide gel containing 7 M urea, dried, and autoradiographed. Yeast tRNA was used as control.

Generation of iPPase Luciferase Reporter Constructs

Different iPPase promoter fragments were generated by PCR using sets of sense primers that had a *Kpn*I site linked to the 5′-end and a common antisense primer containing a *Hin*dIII site linked to its 5′-end. The 1091-bp pGEM-T cloned iPPase promoter fragment was used as template for all the PCR reactions. Three different PCR products (1091, 685, and 335 bp) were obtained using different sense primers: KIPF$_2$ (−1009 to −994; 5′-GG**GGTACC**ATAGTCT CATACTGGA-3′), KIPF$_1$ (−603 to −589; 5′-GG**GG TACC**AGTCCAACAATCCAGA-3′), KIPF (−253 to −238; 5′-GG**GGTACC**TAACTAGCGCTCTGTC-3′), and the common antisense primer HIPR (+82 to +67; 5′-CCC**AAGCTT**GGTGTCCGAGATGTGC-3′), respectively, in which the restriction site has been represented by bold letter and protected nucleotide by underline. The PCR amplification was carried out for 35 cycles using step cycle 94°C for 1 min, 63°C for 1 min, 68°C for 2 min followed by a final extension at 68°C for 8 min, taking 1 unit of platinum *Taq* DNA polymerase. These PCR products were digested with *Kpn*I and *Hin*dIII, gel eluted, and subsequently cloned into the *Kpn*I/*Hin*dIII site of pGL3 basic reporter vector (Promega). All the constructs were sequenced by automated DNA sequencer and were found to be in-frame with the reporter luciferase gene. The three iPPase reporter constructs thus generated were named LucIP −1009/+82, LucIP −603/+82, and LucIP −253/+82.

Transcription Factor Database Search

Transcription factor database search (TFSEARCH, Japan) was performed for the 1009-bp iPPase promoter fragment present in LucIP −1009/+82 reporter construct to identify the different putative transcription factor binding sites on this promoter.

Transient Transfection and Luciferase Assay

Transient transfections were carried out using RAG cells (mouse renal adenocarcinoma cell line). The cells were plated at a density of 2×10^5 cells per well in a six-well plate, 18 h before transfection. For transient transfection 2 μg of respective reporter plasmid DNA and 0.5 μg of pSV-β-gal control vector (Pro-

```
                                                       Cap                    ADR1
-1009  ATAGTCTCATACTGGAGCTCAGGCTGGTCTCAGAACTCAGCTTCCTGAGGTCTGGGGTTATAG

-946  GTAACTTGAGAGTCGTGTTATACACACGAAGAGAGAGAGAGAGAGAGAGAGAGAGAGAGAGAGA
                        HSF                                   Cap
-884  GAGAGAGAGAGAGAGACTCTGAGAAAGTTAGCATGTCCGCAGCGTCACACTCGGGAGGGGTG

-822   GAGTCTGGCCTGAGGTGGTTCAATAGAAGGAAAACAAGCTCCAAGAAGCTACTCCGGAGATA
                                  NFkB                    Cap
-780  TGTCCTCAAGGGGTTCTGAGCACACTCCTGGGCCTTCCCAGAGCTTCAGTGTCAAATCCCAGAG
                AP-1                          GATA-2
-696  GATCTGAAGTGCCTCAGCAAGGAACTGGGTGGGGAGAGATAGCTGCAGTAACTGGGGAGGGC
                                        Sox-5           HSF
-634  AGGAATAATCGGCTTGACACTGGTCCAGGCAGTCCAACAATCCAGATGAGAAACCGAATCAG
              Dfd                                              CCAAT
-572  GGAGATTAGTAAAGCAAATGTGCCCAATGTCTATCACTTGGAAAAACAGAAGTCACAGCCAAT
                                                    ADR1    ADR1
-509  AGTTTTCAGAGCCTAGTCAGCCAAACCCCCAACTAAAATAAAGGCTGCTTGGGGCTGGGGGG
                                          Lyf-1                  NIT2
-447  TTGTTGTTGTTGTTGGTGTTAGTATATTCCCAGCATTTGGGAGGCTGAGGGAGATGAATATCTT

-383  TGAGAAACCCTGTCTCGAAAATTCAAAAAAGAAAGGAGGTGACTTATCAGGGCCTTCTGAGAT
         GATA-3                          AP-1          SRY              StuAp
-320  AAGGAATTGCTCCGAATGATGTGACTGAGTGGAATCAAAGGTGAGTGATTCGCGAGCCTTTGG
                                          P
-257  AGAATAACTAGCGCTCTGTCCCGGTGTAGCCACCAACCGGCTGTCAGCTTCCAGAGGGCAGCC
              USF                              ADR1      Sp1
-194  GGCGCCGGCCTCGTGGCCAAGGTTGGGAGCCTGGGCTGTACTGGGGGCGGGGCGTGAGGAGGC
                                                Sp1
-131  TCGTCGGGAAGAGTGCGCCTGCGCGGATGGACGGGGCGGGGCAGGGTGCAAGGCGAGCCCCA
                                    AP-4                      GCR1
-69  TGCGTTAAAGGCAAGGCGCAGGCGACCAGCGGGCCAGCTCGTGGTGCGCAGGCGCGAGCTTCC
          _              ┌─ +1 (TSS)
-6   TCCACGGTACAACCACTCCGAAGCTGGGCTGTGTGGTTGTGTAGCTGTGCAGCGGCGGCGACG

GCGGCACAGGCACATCTCGGACACC +82
```

Figure 4. Rat liver cytosolic inorganic pyrophosphatase 1009-bp promoter sequence. Nucleotide sequence of iPPase 1009-bp promoter fragment beyond translational start site showing transcription start site (TSS) and putative transcription factor binding sites. This sequence has been deposited in the GenBank with the accession number DQ978330.

mega) was transfected into these cells using lipofectamine reagent (Invitrogen). After 24 h posttransfection, the cells were harvested, lysed, centrifuged, and the lysate was used for luciferase assay using the luciferase assay system (Promega). The colorimetric β-galactosidase assay was performed using standard protocol (20) and luciferase activity was divided by the β-galactosidase activity to normalize for transfection efficiency. All the transfections were repeated in triplicates and the results were expressed as the mean ± SD of three independent experiments. The relative luciferase activity for the construct showing the highest activity was taken as 100% and all the comparisons were made relative to that.

Electrophoretic Mobility Shift Sssay (EMSA)

To confirm the transcription factor database search result, protein–DNA interaction studies for a few important putative transcription factor binding sites on iPPase promoter was carried out. Oligonucleotide du-

plexes corresponding to the identified putative transcription factor binding sites for NF-κB and Sp1 were synthesized (Table 1). For each site, one strand was end-labeled with [γ-^{32}P]ATP using T_4 polynucleotide kinase and annealed to its unlabeled complementary strand. Rat liver nuclear extract (RLNE) was prepared according to the protocol of Terzic et al. (27). EMSA was carried out using a standard protocol (25). Briefly, nuclear extracts (10 μg) were incubated with 20 fmol of radiolabeled oligonucleotide duplex and 0.5–1.0 μg poly(dI-dC) in 20 μl reaction mixture containing 10 mM Tris-HCl, pH 7.5, 50 mM NaCl, 1 mM EDTA, 1 mM DTT, 5% glycerol for 20 min at room temperature. In competition experiments, the unlabeled competitor DNA (100-fold molar excess) was included during the preincubation period. Free DNA and protein-bound DNA complexes were separated on a 5% nondenaturing polyacrylamide gel in 0.5× TBE. After electrophoresis, gels were blotted onto filter papers, dried, and autoradiographed.
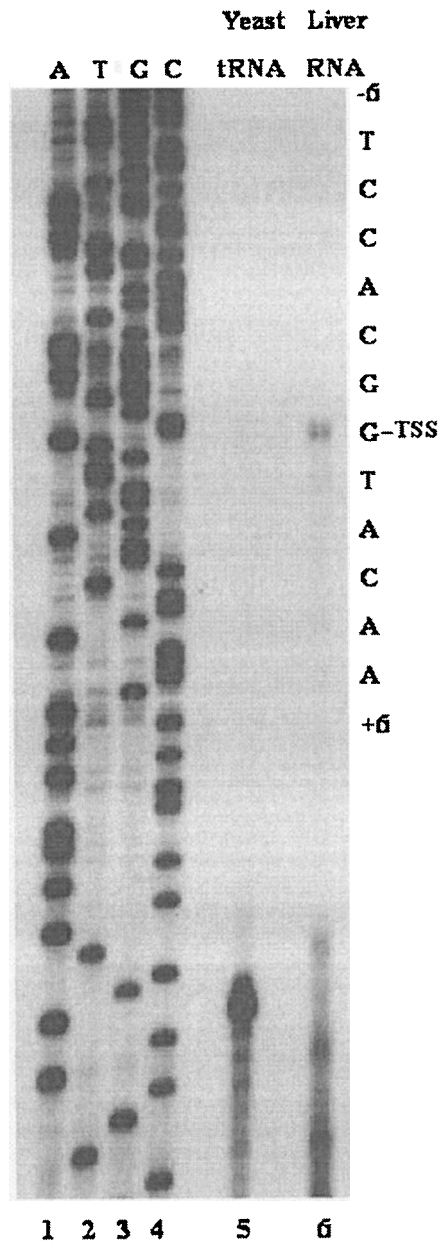
Figure 5. Identification of transcription start site of inorganic pyrophosphatase gene by primer extension analysis. Lanes 1–4, sequencing reactions; lane 5, primer extension product of yeast tRNA; lane 6, primer extension product of liver total RNA. The sequence corresponding to the transcription start site has been marked by a line and is complementary to the sequencing reactions shown in the figure.

RESULTS

Cloning, Expression, and In-Gel Analysis of Rat Liver Cytosolic iPPase

Using primers designed from predicted iPPase mRNA sequence, we obtained a 879-bp RT-PCR product. Sequencing of this 879-bp DNA revealed that its

870-bp sequence showed 100% sequence identity with the complete coding region of predicted rat inorganic pyrophosphatase mRNA (GenBank accession number XM_215416.2) and 93% sequence identity with the mouse breast inorganic pyrophosphatase mRNA (Gen bank accession number BC010468). Further, comparative sequence analysis revealed that this sequence had 100%, 88%, and 87% sequence identity with rat prostate (GenBank accession number BC099794), bovine retina (GenBank accession number M95283), and human uterus inorganic pyrophosphatase mRNA (Gen Bank accession number BC061581), respectively. Further, this 879-bp RT-PCR product was cloned into pTrcHis TOPO TA expression vector and IPTG induced to express the recombinant protein in *E. coli* cells followed by its Ni-NTA column purification under denaturing condition. As expected, a recombinant protein of ~37 kDa was expressed in which the N-terminal peptide containing 6× His-tag was of ~4 kDa and the iPPase protein itself was ~33 kDa (31), as confirmed by SDS-PAGE (Fig. 1) and Western blot analysis (Fig. 2). The bacterial lysate containing recombinant protein and the purified renatured iPPase was checked for enzyme activity by in-gel assay (Fig. 3), which indicated that it is functionally active just as the native liver cytosolic iPPase.

Genomic Organization of Rat Liver Cytosolic iPPase

The genome blast result indicated that this gene is present on chromosome number 20. It consists of 11 exons, 10 introns, and the predicted exon-1 is 192 bp in length. We have cloned and sequenced the proximal 1091-bp sequence upstream of the translational start site, which is expected to be the functional promoter (Fig. 4) of the iPPase gene.

Identification of Transcription Start Site

Primer extension analysis using primer IPER, which is complementary to the +82 to +62 region of iPPase predicted exon-1, established that the transcription start site (Fig. 5) is 82 bp upstream of the translational start site (ATG).

Functional Analysis of iPPase Reporter Constructs

We have analyzed the functional activity of three iPPase promoter–reporter constructs (LucIP −253/+82, LucIP −603/+82, and LucIP −1009/+82) by transient transfection and luciferase reporter assay. Luciferase assay result indicated that among these constructs LucIP −253/+82 has ~1.82-fold and ~2.54-fold more relative luciferase activity than that of LucIP −603/+82 and LucIP −1009/+82, respec-
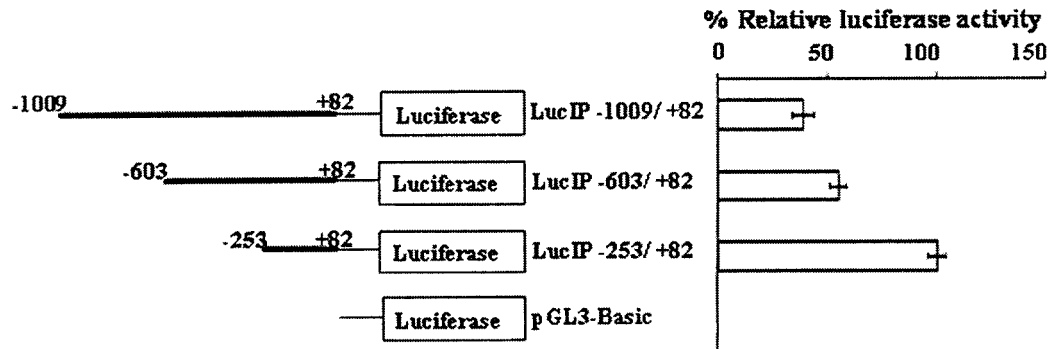
Figure 6. Functional analysis of iPPase promoter by luciferase assay. Relative luciferase activity of different iPPase promoter–reporter constructs was obtained by dividing the luciferase activity by the β-galactosidase activity for normalization of transfection efficiency. All the transfections were repeated in triplicate and the results were expressed as the mean ± SD of three independent experiments. The relative luciferase activity for the construct showing highest activity is taken as 100% and all the comparisons are made relative to this.

tively (Fig. 6). pGL3 basic vector showed negligible luciferase activity compared to these constructs. All these data indicate that these are functional promoter fragments of rat liver cytosolic iPPase gene.

Transcription Factor Binding Search for LucIP −1009/+82 Reporter Construct

The iPPase reporter construct LucIP −1009/+82 contained 1009 bp of iPPase promoter sequence and transcription factor database search for this sequence demonstrated that this is a TATA-less promoter and has multiple Sp1 transcription factor binding sites present proximal to the transcription start site, suggesting an important role of this transcription factor in driving the promoter. Several other transcription factors like GCR1, AP-4, ADR1, USF, P, AP-1, SRY, StuAp, GATA-3, NIT2, Lyf-1, CCAAT, Dfd, Sox-5, GATA-2, NF-κB, Cap, and HSF binding sites were also found on this promoter (Fig. 4). Interestingly, reporter gene assay showed that iPPase promoter–reporter construct LucIP −603/+82 has 1.82-fold less reporter activity than that of LucIP −253/+82 and we speculate that repressor element(s) may be binding to the −253 to −658 region of this construct and regulating the reporter gene activity. However, further experiments will confirm which of the above transcription factors are actually binding to the promoter and their exact role in regulating the expression of rat liver cytosolic iPPase.

Electrophoretic Mobility Shift Assay

Protein–DNA interaction studies for the two proximal Sp1 sites (−102 to −82 and −158 to −138) and NF-κB binding site (−736 to −717) revealed that these transcription factors are interacting with this promoter as they form specific complexes with their respective labeled oligonucleotide duplexes. Compe-

tition with 100-fold molar excess of unlabeled homologous self-DNA and consensus oligonucleotide duplexes for respective transcription factor binding sites abolished the complex formation, whereas the complex was not competed with an oligonucleotide duplex corresponding to the nonspecific transcription factor binding site (SRY), indicating the specificity of these protein–DNA interactions (Fig. 7).

DISCUSSION

In the liver, besides a few of the regular biochemical reactions like DNA synthesis [through the action of DNA polymerase (EC 2.7.7.7)] and amino acid activation [through the action of a number of specific ligases forming aminoacyl-tRNA (EC 6.1.1.1)], there are several other specific biochemical reactions like glycogen synthesis, fat metabolism, and urea synthesis (7) that generate large amounts of PPi. PPi exhibits end product inhibition for certain enzymes like aminoacyl tRNA synthetase (13) and also has high affinity for divalent metal ions like Mg^{2+}, Ca^{2+}, and Fe^{2+}, thus acting as a natural chelator in vivo, thereby regulating those biochemical reactions in which these metal ions are involved. Therefore, the hydrolysis of PPi by inorganic pyrophosphatase enzyme is a crucial thermodynamic force for driving several biochemical reactions in the forward direction (12). In the liver PPi hydrolysis is mainly carried out by cytosolic inorganic pyrophosphatase, which is very important from a physiological point of view because it controls the steady-state level of intracellular PPi, thereby directly or indirectly regulating several metabolic processes.

The elevation of PPi and PPi-generating nucleoside triphosphate pyrophospho-hydrolase (NTPPPH) has been reported with aging (10). Besides NTPPPH,
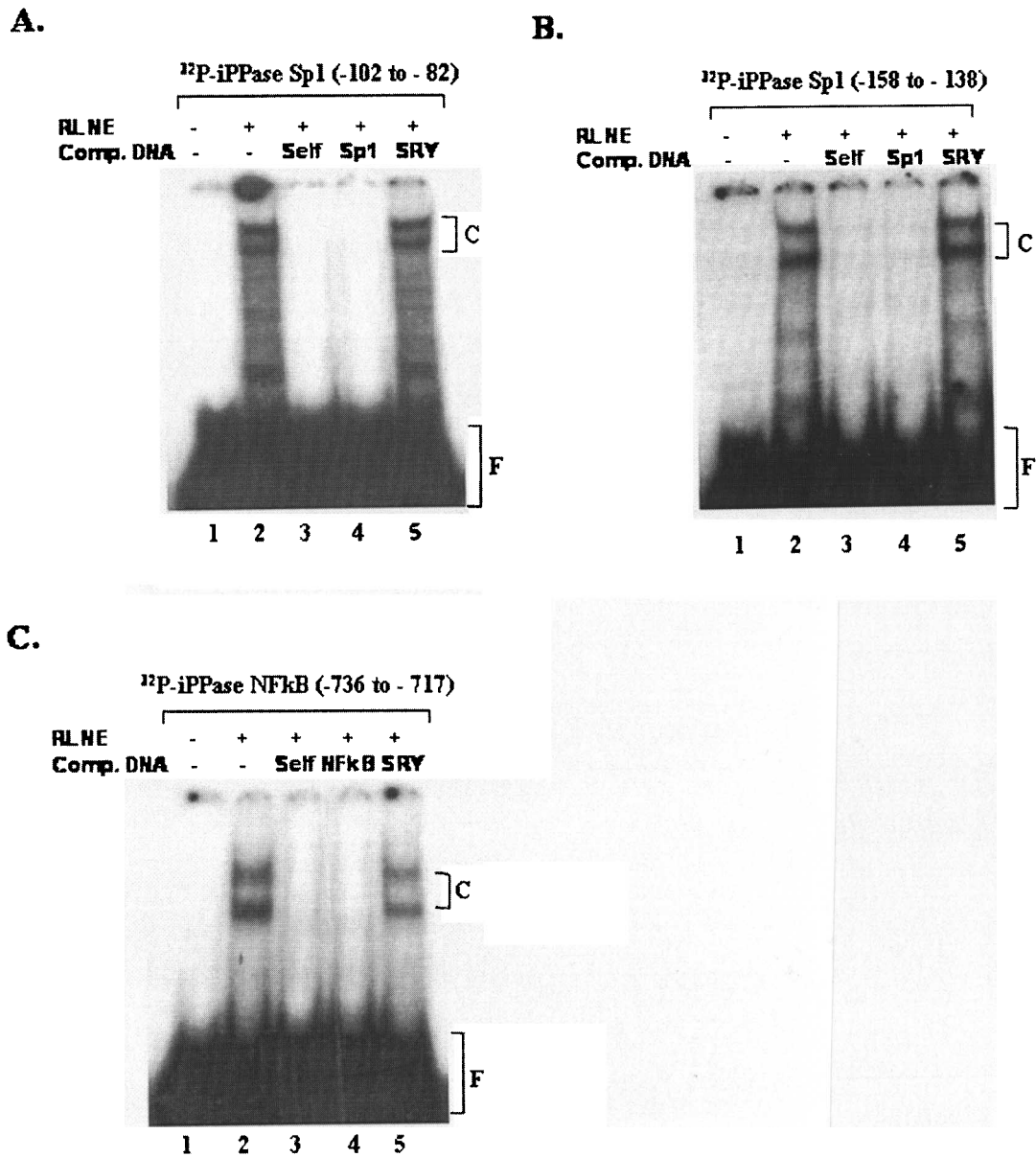
A.

B.

C.

Figure 7. Protein–DNA interaction studies. Electrophoretic mobility shift assay (EMSA) for Sp1 site (−102 to −82) (A), Sp1 site (−158 to −138) (B), and NF-κB site (−736 to −717) (C) on iPPase promoter. Lane 1, labeled oligonucleotide duplex without nuclear extract; lanes 2–5, labeled oligonucleotide duplex with 10 μg rat liver nuclear extract (RLNE). Lane 2, no competitor DNA; lane 3, 100-fold molar excess of unlabeled homologous self (corresponding to the particular binding site) oligonucleotide duplex; lane 4, 100-fold molar excess of unlabeled consensus oligonucleotide duplex; lane 5, 100-fold molar excess of unlabeled nonspecific oligonucleotide duplex (SRY). C and F denote the positions of protein–DNA complex and free probe, respectively.

several other transcripts encoding enzymes participating in oxidation of glucose, fatty acids, and lipogenesis have been found to be increased in old rat liver, leading to more PPi generation (28). The differential expression of iPPase in old liver could be because of major metabolic burden of PPi accumulation during aging and may be a physiological adaptation associated with maintenance of steady-state level of intracellular PPi, which, directly or indirectly, regulates

several metabolic processes. In mammals the iPPase is a homodimer protein and consists of two identical subunits. In rat liver, there are reports of two different inorganic pyrophosphatase—one form having two identical subunits of ∼30–33 kDa each (31) and the other one having two 38-kDa subunits (24), suggesting the expression of two different isoforms.

In the present study, we cloned, expressed, and analyzed the functional activity of this ∼33 kDa rat cy-

tosolic inorganic pyrophosphatase protein and confirmed the existence of ~30–33 kDa isoform. Further, we elucidated for the first time, to our knowledge, the genomic organization of this gene by genome blast approach, cloned and characterized its proximal 1009-bp functional promoter (−1009 to +82) by transient transfection and luciferase assay of different 5′-deleted iPPase promoter–luciferase constructs, its transcription start site, putative transcription factor binding sites, and also carried out protein–DNA interaction studies for a few putative transcription factor binding sites. Protein–DNA interaction studies revealed the binding of Sp1 transcription factor to the proximal Sp1 sites (−102 to −82 and −158 to −138) on this TATA-less promoter, thus strengthening our assumption that it may be involved in driving this promoter, as binding of Sp1 to *cis*-regulatory elements located in the proximal region of TATA-less promoters have been widely reported to contribute to the basal promoter activity (5,22).

Interestingly, we found protein–DNA interaction for the NF-κB site (−736 to −717) on this promoter.

NF-κB) is a ubiquitously expressed, highly inducible transcription factor that has been reported as a transcriptional activator for several genes, especially those involved in immune response, inflammation, and apoptosis (1–3,30). NF-κB undergoes age-associated increase in its DNA binding activity (25) and has been shown to be involved in upregulation of several genes with aging (11,14,32). Here we speculate that the increased expression of rat liver cytosolic iPPase may be coordinated by the age-associated increased binding of NF-κB to its promoter and has an important role to play in the transcriptional regulation of this gene during aging.

ACKNOWLEDGMENTS

REFERENCES

1. Baeuerle, P. A.; Henkel, T. Function and activation of NF-kappa B in the immune system. Annu. Rev. Immunol. 12:141–179; 1994.
2. Baeuerle, P. A.; Baltimore, D. NF-kappa B: Ten years after. Cell 87:13–20; 1996.
3. Barkett, M.; Gilmore, T. D. Control of apoptosis by Rel/NF-kappaB transcription factors. Oncogene 18:6910–6924; 1999.
4. Davidson, A. M.; Halestrap, A. P. Inorganic pyrophosphate is located primarily in the mitochondria of hepatocyte and increases in parallel with the decrease in light-scattering induced by gluconeogenic hormones, butyrate and ionophore A23187. Biochem. J. 254:379–384; 1988.
5. Dusing, M. R.; Wiginton, D. A. Sp1 is essential for both enhancer-mediated and basal activation of the TATA-less human adenosine deaminase promoter. Nucleic Acids Res. 22:669–677; 1994.
6. Gupta, A.; Amin, N. B.; Besarab, A.; Vogel, S. E.; Divine, G. W.; Yee, J.; Anandan, J. V. Dialysate iron therapy: infusion of soluble ferric pyrophosphate via the dialysate during hemodialysis. Kidney Int. 55:1891–1898; 1999.
7. Guynn, R. W.; Veloso, D.; Lawson, J. W. R.; Veech, R. L. The concentration and control of cytoplasmic free inorganic pyrophosphate in rat liver in vivo. Biochem. J. 140:369–375; 1974.
8. Hager, D. A.; Burgess, R. R. Elution of proteins from sodium dodecyl sulfate-polyacrylamide gels, removal of sodium dodecyl sulfate, and renaturation of enzymatic activity: Results with sigma subunit of *Escherichia coli* RNA polymerase, wheat germ DNA topo-

isomerase, and other enzymes. Anal. Biochem. 109:76–86; 1980.
9. Horn, A.; Bornig, H.; Thiele, G. Allosteric properties of the Mg^{++}-dependent inorganic pyrophosphatase in mouse liver cytoplasm. Eur. J. Biochem. 2:243–249; 1967.
10. Johnson, K.; Pritzker, K.; Goding, J.; Terkeltaub, R. The nucleoside triphosphate pyrophosphohydrolase isozyme PC-1 directly promotes cartilage calcification through chondrocyte apoptosis and increased calcium precipitation by mineralizing vesicles. J. Rheumatol. 28:2681–2691; 2001.
11. Kim, H. J.; Kim, K. W.; Yu, B. P.; Chung, H. Y. The effect of age on cyclooxygenase-2 gene expression: NF-kappaB activation and IkappaBalpha degradation. Free Radic. Biol. Med. 28:683–692; 2000.
12. Kornberg, A. On the metabolic significance of phosphorolytic and pyrophosphorolytic reactions. In: Kasha, M.; Pullman, B., eds. Horizons in biochemistry. New York: Academic Press, Inc.; 1962:251–264.
13. Lahti, R. Microbial inorganic pyrophosphatases. Microbiol. Rev. 47:169–178; 1983.
14. Lavrovsky, Y.; Song, C. S.; Chatterjee, B.; Roy, A. K. Age-dependent increase of heme oxygenase-1 gene expression in the liver mediated by NFkappaB. Mech. Ageing Dev. 114:49–60; 2000.
15. Mansurova, S. E. Inorganic pyrophosphate in mitochondrial metabolism. Biochim. Biophys. Acta 977:237–247; 1989.
16. Michels, P. A.; Chevalier, N.; Opperdoes, F. R.; Rider, M. H.; Rigden, D. J. The glycosomal ATP-dependent phosphofructokinase of *Trypanosoma brucei* must

have evolved from an ancestral pyrophosphate-dependent enzyme. Eur. J. Biochem. 250:698–704; 1997.

17. Nordlie, R. C.; Arion, W. J. Liver microsomal glucose 6-phosphatase, inorganic pyrophosphatase, and pyrophosphate-glucose phosphotransferase.3. Associated nucleoside triphosphate-and nucleoside diphosphate-glocose phosphotransferase activities. J. Biol. Chem. 240:2155–2164; 1965.

18. Panda, H.; Pandey, R. S.; Debata, P. R.; Supakar, P. C. Age-dependent differential expression and activity of rat liver cytosolic inorganic pyrophosphatase gene. Biogerontology (in press).

19. Rachow, J. W.; Ryan, L. M. Inorganic pyrophosphate metabolism in arthritis. Rheum. Dis. Clin. North Am. 14:289–302; 1988.

20. Sambrook, J.; Fritsch, E. F.; Maniatis, T. Molecullar cloning: A laboratory manual, 2nd ed. Cold Spring Harbor: Cold Spring Harbor Laboratory Press; 1989.

21. Shatton, J. B.; Williams, A.; Weinhouse, S. Subcellular distribution of inorganic pyrophosphatase activity in various normal and neoplastic cell types. Cancer Res. 43:3742–3747; 1983.

22. Shimakura, J.; Terada, T.; Katsura, T.; Inui, K. Characterization of the human peptide transporter PEPT1 promoter: Sp1 functions as a basal transcriptional regulator of human PEPT1. Am. J. Physiol. Gastrointest. Liver Physiol. 289:G471–G477; 2005.

23. Simonovic, A. D.; Gaddameedhi, S.; Anderson, M. D. In-gel precipitation of enzymatically released phosphate. Anal. Biochem. 334:312–317; 2004.

24. Smirnova, I. N.; Baikov, A. A. Inorganic pyrophosphatase of rat liver cytosol. Isolation and properties. Biokhimiia 54:228–234; 1989.

25. Supakar, P. C.; Roy, A. K. Role of transcription factors in the age-dependent regulation of the androgen receptor gene in rat liver. Biol. Signals 5:170–179; 1996.

26. Terkeltaub, R. A. Inorganic pyrophosphate generation and deposition in patho-physiology. Am. J. Physiol. Cell Physiol. 281:C1–C11; 2001.

27. Terzic, N.; Vujcic, M.; Ristic-Fira, A.; Krstic-Demonacos, M.; Milanovic, D.; Kanazir, D. T.; Ruzdijic, S. Effects of age and dexamethasone treatment on glucocorticoid response element and activating protein-1 binding activity in rat brain. J. Gerontol. A Biol. Sci. Med. Sci. 58:297–303; 2003.

28. Tollet-Egnell, P.; Flores-Morales, A.; Stahlberg, N.; Malek, R. L.; Lee, N.; Norstedt, G. Gene expression profile of the aging process in rat liver: Normalizing effects of growth hormone replacement. Mol. Endocrinol. 15:308–318; 2001.

29. Weaver, J.; Zhan, H.; Pollack, S. Mitochondria have Fe (III) receptors. Biochem. J. 265:415–419; 1990.

30. Wu, D.; Meydani, S. N. Mechanism of age-associated up-regulation in macrophage PGE2 synthesis. Brain Behav. Immun. 18:487–494; 2004.

31. Yoshida, C.; Shah, H.; Weinhouse, S. Purification and properties of inorganic pyrophosphatase of rat liver and hepatoma 3924A. Cancer Res. 42:3526–3531; 1982.

32. Zhang, J.; Johnston, G.; Stebler, B.; Keller, E. T. Hydrogen peroxide activates NFkappaB and the interleukin-6 promoter through NFkappaB-inducing kinase. Antioxid. Redox Signal. 3:493–504; 2001.